Am J Physiol Regul Integr Comp Physiol 316: R687–R696, 2019.
First published March 20, 2019; doi:10.1152/ajpregu.00192.2018.

RESEARCH ARTICLE | *Translational Physiology*

P2X7 receptor deletion suppresses γ-radiation-induced hyposalivation

Kristy E. Gilman,[1] Jean M. Camden,[2] Rob R. Klein,[3] Qionghui Zhang,[1] Gary A. Weisman,[2] and Kirsten H. Limesand[1]

[1]*Department of Nutritional Sciences, The University of Arizona, Tucson, Arizona;* [2]*Christopher S. Bond Life Sciences Center, Department of Biochemistry, The University of Missouri, Columbia, Missouri; and* [3]*Department of Pathology, The University of Arizona, Tucson, Arizona*

Submitted 25 June 2018; accepted in final form 4 March 2019

Gilman KE, Camden JM, Klein RR, Zhang Q, Weisman GA, Limesand KH. P2X7 receptor deletion suppresses γ-radiation-induced hyposalivation. *Am J Physiol Regul Integr Comp Physiol* 316: R687–R696, 2019. First published March 20, 2019; doi:10.1152/ajpregu.00192.2018.—Head and neck cancer treatments typically involve a combination of surgery and radiotherapy, often leading to collateral damage to nearby tissues causing unwanted side effects. Radiation damage to salivary glands frequently leads to irreversible dysfunction by poorly understood mechanisms. The P2X7 receptor (P2X7R) is a ligand-gated ion channel activated by extracellular ATP released from damaged cells as "danger signals." P2X7R activation initiates apoptosis and is involved in numerous inflammatory disorders. In this study, we utilized P2X7R knockout ($P2X7R^{-/-}$) mice to determine the role of the receptor in radiation-induced salivary gland damage. Results indicate a dose-dependent increase in γ-radiation-induced ATP release from primary parotid gland cells of wild-type but not $P2X7R^{-/-}$ mice. Despite these differences, apoptosis levels are similar in parotid glands of wild-type and $P2X7R^{-/-}$ mice 24–72 h after radiation. However, γ-radiation caused elevated prostaglandin E_2 (PGE_2) release from primary parotid cells of wild-type but not $P2X7R^{-/-}$ mice. To attempt to uncover the mechanism underlying differential PGE_2 release, we evaluated the expression and activities of cyclooxygenase and PGE synthase isoforms. There were no consistent trends in these mediators following radiation that could explain the reduction in PGE_2 release in $P2X7R^{-/-}$ mice. Irradiated $P2X7R^{-/-}$ mice have stimulated salivary flow rates similar to unirradiated controls, whereas irradiated wild-type mice have significantly decreased salivary flow rates compared with unirradiated controls. Notably, treatment with the P2X7R antagonist A438079 preserves stimulated salivary flow rates in wild-type mice following γ-radiation. These data suggest that P2X7R antagonism is a promising approach for preventing γ-radiation-induced hyposalivation.

cell biology; P2X7 receptor; P2X7R; radiation; salivary glands; xerostomia

INTRODUCTION

It is anticipated that over 60,000 new cases of head and neck cancer will be diagnosed in the United States annually (26) and treated with a combination of surgery, γ-radiation, and chemotherapy. Radiation therapy for head and neck cancer frequently results in salivary gland dysfunction and xerostomia that leads to mucositis, dental caries, malnutrition, and an overall decreased quality of life (8). Currently, there are few viable approaches to prevent γ-radiation-induced salivary gland damage, and a better understanding of the mechanisms involved could lead to more effective treatments for these patients.

The ubiquitously expressed P2X7 receptor (P2X7R) for ATP can regulate various biological processes, including inflammation, neuromodulation, muscle tone, cell proliferation, and cell death (27, 31). The P2X7R is a member of the P2X purinoceptor family composed of extracellular ATP (eATP)-gated ion channels that require >100 μM eATP for activation (31), levels that occur in inflammation, injury, or disease and act as "danger signals" to neighboring cells (16). P2X7R activation by eATP triggers the opening of nonselective cation channels that depolarize the plasma membrane and, when sustained, initiate the formation of plasma membrane pores that facilitate the efflux of cytoplasmic nucleotides and other hydrophilic molecules into the extracellular space (16, 25, 30). P2X7R activation also leads to the release of eicosanoids, cytokines, and exosomes and frequently results in cell apoptosis (1, 29), including in salivary epithelial cells (10, 32). Apoptosis of salivary epithelial cells is a well-described mechanism of γ-radiation-induced salivary gland dysfunction (4, 15, 18).

The P2X7R plays a role in inflammation, immune cell recruitment, and removal of damaged cells (7, 10, 31). P2X7R activation leads to the production and secretion of proinflammatory signals, including the release of the eicosanoid prostaglandin E_2 (PGE_2) (5, 9) and cytokines, including interleukin-1β (IL-1β), IL-6, IL-18, and tumor necrosis factor-α (TNF-α), often through formation of the NLRP3 inflammasome (10, 11, 16). The P2X7R is a major contributor to inflammatory diseases, such as rheumatoid arthritis (RA), inflammatory bowel disease, and pulmonary fibrosis (3). In patients with RA, eATP is found in synovial fluid between joints and is hypothesized to induce production of inflammatory cytokines, tissue damage, and continued release of eATP (16). The P2X7R may also play a role in radiation-induced brain injury (RBI), where increased eATP levels within cerebrospinal fluid in humans and mice were positively correlated with the severity of RBI (35). Xu et al. (35) also observed elevated TNF-α and IL-6 levels in those receiving radiation treatment compared with controls.

The P2X7R has been evaluated as a potential therapeutic target in a variety of diseases and tissue types, but its impact on salivary gland dysfunction after radiation has not been previously studied. Here, we utilized P2X7R knockout mice to examine the role of the P2X7R in salivary gland dysfunction following γ-radiation. Given the well-established role of P2X7Rs in mediating apoptosis and inflammatory responses,

Address for reprint requests and other correspondence: K. H. Limesand, 1177 E. 4th St., Shantz 421, Tucson, AZ 85721 (e-mail: limesank@u.arizona.edu).

we examined the possibility that P2X7R-deficient ($P2X7R^{-/-}$) mice would exhibit decreased radiation-induced cell apoptosis and increased saliva production, as compared with irradiated control mice.

MATERIALS AND METHODS

Ethics statement. All mice were housed and maintained in accordance with the University of Arizona Institutional Animal Care and Use Committee. All protocols were approved by the Institutional Animal Care and Use Committee.

Mice. C57BL/6J mice (wild-type, stock no. 000664), B6.129P2-P2rx7^{tm1Gab}/J mice ($P2X7R^{-/-}$, stock no. 005576), and FVB/NJ mice (wild type; stock no. 001800) were purchased from Jackson Laboratories (Bar Harbor, ME). Animals were housed in vented cages with 12-h light-dark cycles and ad libitum access to food and water. Age and size matched 4- to 8-wk-old mice were assigned to treatment groups for all experiments via block randomization. Health of the animals was evaluated by body weight changes throughout the study. $P2X7R^{-/-}$ mice were genotyped, as previously described (20) with $P2X7R^{-/-}$-specific (5′-GCC AGA GGC CAC TTG TGT AG-3′) or wild-type-specific (5′-TCA CCA CCT CCA AGC TCT TC-3′) and common (5′-TAT ACT GCC CCT CGG TCT TG-3′) primers (Integrated DNA Technologies, Coralville, IA).

Radiation treatment. Four- to eight-week-old female C57BL/6J, FVB or $P2X7R^{-/-}$ mice were sedated via intramuscular injection of a ketamine-xylazine mixture (70 mg/kg-10 mg/ml) before irradiation. Mice were then constrained in 50-ml conical tubes and shielded with >6 mm lead with only their head and neck region exposed to a single dose of 5 Gy of irradiation (^{60}Co Teletherapy unit, Theratron-80; Atomic Energy of Canada; 80-cm distance from source, ~0.5 Gy/min). For single-dose antagonist experiments, FVB mice were injected intraperitoneally with the P2X7R antagonist A438079 (70 mg/kg body wt; TOCRIS, Minneapolis, MN) or sterile saline (vehicle) 1 h before radiation exposure (10, 33). For multidose antagonist experiments, FVB mice were injected intraperitoneally with A438079 (70 mg/kg body wt) or sterile saline 1 h before radiation exposure and again at *days 5* and *10* post-γ-radiation.

Primary cell culture. Parotid glands were removed from four-eight week-old male or female $P2X7R^{-/-}$ or C57BL/6J mice, minced for 2–3 min, and added to a siliconized Erlenmeyer flask with 30 ml dispersion media (Hank's salt solution, 1 mg/ml collagenase, and 1 mg/ml hyaluronidase, pH 7.4). Cells were incubated in a shaking water bath at 37°C for 1 h with mechanical agitation at 40, 45, 50, 55, and 60 min. Cells were then centrifuged, resuspended in wash media [modified Hank's solution containing $CaCl_2$ and 0.2% (wt/vol) BSA], recentrifuged, and resuspended again. The suspension was run through a sterile funnel filter, recentrifuged, and suspended in primary cell culture media: DMEM/F12 containing (in wt/vol except where noted) gentamycin (0.5%; Fisher Scientific), fungizone (0.2%; Invitrogen), hydrocortisone (0.04%; Sigma-Aldrich), EGF (0.4%; Fisher Scientific), insulin (0.125%; Invitrogen), transferrin (0.125%, Invitrogen), retinoic acid (0.05%; Sigma-Aldrich), glutamine (1.25%; Invitrogen), nonessential amino acids (1%; Invitrogen), trace elements (1%; Fisher Scientific), and fetal bovine serum (10% vol/vol; Fisher Scientific). Cells were plated on 35-mm rat tail collagen plates (stock no. 08-772-73, Corning, Corning, NY) and grown for 3 days. One mouse supplies an adequate number of cells for two primary cell culture plates. One plate from each independent primary cell culture preparation is considered a replicate for assays involving the use of primary cells.

ATP release assay. Primary parotid cells were exposed to 2, 5, or 10 Gy of radiation (80-cm distance from source, ~0.5 Gy/min), and supernatants were collected immediately following γ-radiation. For antagonist experiments, cells were treated with 25 μM A438079 (half-life: 1 h; Ref. 19) or sterile saline mixed in DMEM/F12 for 1 h before γ-radiation treatment (10). The eATP concentration was measured with an ATP bioluminescence kit (stock no. 11699695001; Roche, Tucson, AZ) per the manufacturer's instructions and luminescence intensity was measured with a luminometer (Promega GloMax, Madison, WI). ATP concentrations were calculated via a standard curve and normalized to the average of the untreated control from each independent preparation.

Histology. Salivary glands were removed at 24, 48, or 72 h post-γ-radiation, fixed in 10% (vol/vol) formalin for 24 h, and sent to IDEXX Bioresearch (Columbia, MO), where they were transferred to 70% (vol/vol) ethanol, embedded in paraffin, and sectioned into 4-μm sections. One section from each sample was stained with hematoxylin and eosin. A board-certified pathologist who was blinded to treatment groups viewed and analyzed tissue sections from four mice per treatment to determine any morphological alterations in salivary tissue at *day 30* following radiation exposure.

Cleaved caspase-3 staining assay. Parotid tissue sections were incubated at 37°C for 45 min and rehydrated in histoclear (National Diagnostics, Atlanta, GA) with alcohol gradations [100, 95, 70, and 50% (vol/vol) and water] for 10 min each. Slides were microwaved in citric acid (0.01 M, pH 6.8) twice for 5 min and then cooled for 20 min for antigen retrieval. Slides were washed in phosphate-buffered saline (PBS) for 15 min, blocked with ABC Rabbit Kit (catalog no. PK-6101; Vector Laboratories, Burlingame, CA) for 20 min at room temperature and then incubated overnight at 4°C in a 1:100 dilution of anti-cleaved caspase-3 primary antibody (stock no. 9661; Cell Signaling Technology, Danvers, MA). Then, slides were washed in PBS three times for 10 min, in 1% (vol/vol) H_2O_2 (Fisher Scientific, Fair Lawn, NJ) for 5 min to neutralize endogenous peroxidase activity, in PBS twice for 5 min, and then in biotinylated secondary antibody for 50 min at room temperature per the manufacturer's instructions (ABC Rabbit Kit; Vector Laboratories). Finally, slides were washed in PBS three times for 5 min, incubated in ABC Reaction Kit (ABC Rabbit Kit; Vector Laboratories) for 30 min, washed in PBS three times for 5 min each, incubated in DAB (Biogenex Laboratories, Fremont, CA) for 6–8 min to develop positive staining, washed in water to stop the reaction, counterstained with hematoxylin for ~2 s (Sigma-Aldrich, St. Louis, MO), rinsed in water for 10 min, dehydrated in alcohol gradations [50, 70, 95, and 100% (vol/vol)] and histoclear for 10 min each, and mounted with Protocol SecureMount (Fisher Scientific, Kalamazoo, MI). Images were taken using a Leica DM5500 and 4-megapixel Pursuit camera. Cleaved caspase-3-positive cells in parotid sections were manually counted from five images per slide at ×400 magnification with four mice per treatment group and quantified by averaging the number of positive cells out of the total number of cells from five fields of view per mouse. Graphs depict the average number of positive cells/total number of cells.

Terminal deoxynucleotidyl transferase dUTP nick-end labeling assay. Parotid tissue sections were rehydrated in histoclear (National Diagnostics) with alcohol gradations [100, 95, 70, and 50% (vol/vol) and water] for 10 min each. Slides were washed in PBS twice for 5 min, then incubated in the terminal deoxynucleotidyl transferase dUTP nick-end labeling (TUNEL) reaction mixture in a humidified chamber in the dark for 20 min per the manufacturer's instructions (In Situ Cell Death Detection Kit, catalog no. 12156792910, TMR Red; Roche). Slides were rinsed with PBS three times, counterstained with DAPI (1 μg/ml) in the dark for 5 min, rinsed in PBS three times, and mounted with Prolong Gold Antifade Mountant (catalog no. P36934; Thermo Fisher Scientific). Images were taken using a Leica DM5500 and 4-megapixel Pursuit camera. TUNEL-positive cells in parotid sections were manually counted from three images per slide at ×400 magnification with four mice per treatment group and quantified by averaging the number of positive cells out of the total number of cells from three fields of view/mouse. Graphs depict the average number of positive cells/total number of cells.

PGE_2 ELISA. Primary parotid cells were exposed to 5 Gy of radiation (80-cm distance from source, ~0.5 Gy/min), and supernatants were collected at 0, 24, 48, and 72 h post-γ-radiation. For

P2X7R antagonist experiments, cells were treated with 10, 25, or 50 μM A438079 or sterile saline mixed in primary cell culture media, as described above, and the supernatant was collected at 1 or 24 h. PGE_2 content was determined using an ELISA kit (catalog no. KGE004B; R&D Systems Minneapolis, MN) per the manufacturer's instructions, and absorbance was measured with a microplate imaging system (Ultramark EX; Bio-Rad).

RNA isolation and RT-PCR. Parotid glands were removed from P2X7R$^{-/-}$ or wild-type mice at 0, 24, and 48 h after 5 Gy of γ-radiation. Tissues were placed in RNAlater (catalog no. 76106; Qiagen, Hilden, Germany) for 24 h. RNA was isolated with the RNeasy Mini Kit (catalog no. 74104; Qiagen) per the manufacturer's instructions, followed by DNA digestion using the RNase-free DNase set (catalog no. 79254; Qiagen). RNA was diluted to 200 μg/μl for each sample, and cDNA was synthesized using the SuperScript IV First-Strand Synthesis Kit (stock no. 18091050; Invitrogen) with oligo (dT) and 5 μl of diluted RNA per reaction, following the manufacturer's instructions. cDNA was diluted 1:5 and used for subsequent analysis. RT-PCR was performed on the iQ5 Real-Time PCR detection system (Bio-Rad), using the QuantiTect SYBR green PCR Kit (catalog no. 204145; Qiagen), as described previously (18). The following primers were purchased from Integrated DNA Technologies and used for the following: *cyclooxygenase-1* (*COX-1*; forward: 5′-CTC CCA GAG TCA TGA GTC GAA-3′, reverse: 5′-GTC AGC AGG AAA TGG GTG AA-3′), *cyclooxygenase-2* (*COX-2*; forward: 5′-AGC TCG TTG ATG AGT GGT AG-3′, reverse: 5′-CAG CCT GGC AAG TCT TTA AC-3′), *microsomal prostaglandin E synthase-1* (*m-PGES-1*, forward: 5′-GAA GGC TTC TCA GAC CTA CC-3′, reverse: 5′-ACT CAA AGG ACG GTG GTA TC-3′), *microsomal prostaglandin E synthase-2* (*mPGES-2*; forward: 5′-CAG CTC AAT GAC TCC TCT GT-3′, reverse: 5′-GCC TTC ATG GGT GGG TAA TA-3′), and *cytosolic PGE synthase* (*cPGES*; forward: 5′-GCT TAA TTG GCT CAG TGT GG-3′, reverse: 5′-TCT CAA AAT CCA GGC GAT GA-3′). Target genes were normalized to 15S ribosomal RNA (forward: 5′-ACT ATT CTG CCC GAG ATG GTG-3′, reverse: 5′-TGC TTT ACG GGC TTG TAG GTG- 3′; Integrated DNA Technologies) and expressed as fold change compared with the average of data from untreated wild-type mice. The Taqman Mouse Apoptosis Gene Expression Array was used per manufacturer's instructions with synthesized cDNA, as previously described (10).

Cyclooxygenase activity assay. Parotid glands were removed from P2X7R$^{-/-}$ or wild-type mice at 0, 24, and 48 h after 5 Gy of radiation. Tissues were rinsed in PBS and snap-frozen and then homogenized on ice in RIPA buffer with 5 mM sodium vanadate, 100 mM PMSF, and protease inhibitor cocktail (15 μl/ml, catalog no. P8340; Sigma-Aldrich) using a Dounce homogenizer. The homogenate was centrifuged at 12,000 *g* for 3 min at 4°C, and the supernatant was collected and kept on ice. The cyclooxygenase activity assay (catalog no. ab204699; Abcam) was performed per the manufacturer's instructions with 1 μg/μl of protein for each sample.

Saliva collection. Stimulated whole saliva collection was performed on *days 3* and *30* following radiation treatment. Mice were injected intraperitoneally with carbachol (0.25 mg/kg body wt) and whole saliva was collected via vacuum aspiration for 5 min immediately following the injection. Saliva was collected in preweighed tubes and kept on ice. Salivary flow rates were calculated by dividing the difference in tube weight (pre- versus postsaliva collection) by the number of minutes to determine the amount of saliva (mg) per minute of collection. These values were then normalized to the average saliva flow rate of the untreated wild-type group on each day of collection.

Statistical analysis. Statistical analysis was done using SPSS (IBM, Armonk, NY) or GraphPad Prism 6 software (GraphPad Software, La Jolla, CA). Power calculations to determine the sample size necessary to obtain statistically significant results with $\alpha = 0.05$ and $\beta = 0.20$ were performed using preliminary or published data and indicate that in vitro experiments require a minimum of three plates from three independent primary cell preparations per treatment, in vivo experiments require a minimum of four mice per treatment, and salivary flow rate determinations require a minimum of eight mice per treatment. For analysis of ATP release assays, data were normalized to the untreated control from each independent primary cell culture preparation. For analysis of saliva flow rates, data were normalized to the average of the untreated group from each day of saliva collection. The Shapiro-Wilk or the Kolmogorov-Smirnov tests were used to assess normality of data sets. To determine statistical significance between treatment groups, a one-way ANOVA was performed followed by a Bonferroni post hoc test with normally distributed data and the nonparametric Kruskal-Wallis test was performed followed by Dunn's post hoc test for nonnormally distributed data. A $P < 0.05$ is considered to be statistically significant.

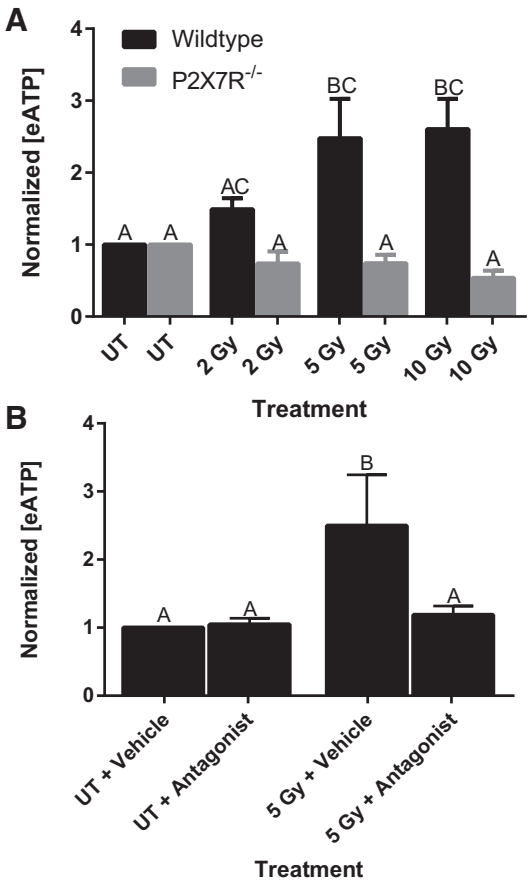

Fig. 1. P2X7 receptor (P2X7R) deletion or inhibition decreases ATP release in irradiated primary parotid gland cells. *A*: parotid gland cells were prepared, as described in MATERIALS AND METHODS, from P2X7R$^{-/-}$ (gray bars) and wild-type mice (black bars) and were untreated (UT, $n = 6$) or exposed to a single dose of 2, 5, or 10 Gy of radiation ($n = 5$ per treatment). *B*: parotid gland cells from wild-type mice were treated with saline (vehicle) or the P2X7R antagonist (A438079, 25 μM) for 1 h before 5 Gy of radiation ($n = 5$ per treatment). The supernatant was collected immediately after γ-radiation and ATP release was measured via a luciferin-luciferase assay. eATP, extracellular ATP. Data are presented as means ± SE. Normality was assessed with the Kolmogorov-Smirnov test. Significant differences between treatments were determined using one-way ANOVA and the Bonferroni post hoc test ($P < 0.05$). Data from treatment groups with the same letters are not significantly different from each other, but groups with different letters are significantly different.

RESULTS

Primary parotid gland cells from P2X7R$^{-/-}$ versus wild-type mice have decreased ATP release post-γ-radiation. The P2X7R is activated by eATP (11), which has been previously shown to be released from keratinocytes following γ-radiation (28). To determine the amount of eATP released from salivary glands postradiation treatment, we evaluated the effect of various radiation doses (2, 5, and 10 Gy) on ATP release from primary parotid gland cells isolated from wild-type or P2X7R$^{-/-}$ mice. The concentration of eATP released from untreated wild-type and P2X7R$^{-/-}$ primary parotid gland cells is not significantly different (Fig. 1*A*). Increasing doses of radiation enhance ATP release from wild-type primary parotid gland cells; however, irradiated P2X7R$^{-/-}$ primary cells have significantly lower eATP levels following 5 and 10 Gy of radiation (Fig. 1*A*, $P < 0.01$). To further validate the role of P2X7R in γ-radiation-induced ATP release, primary parotid gland cells isolated from wild-type mice were pretreated with the P2X7R-selective antagonist A438079 (25 μM)

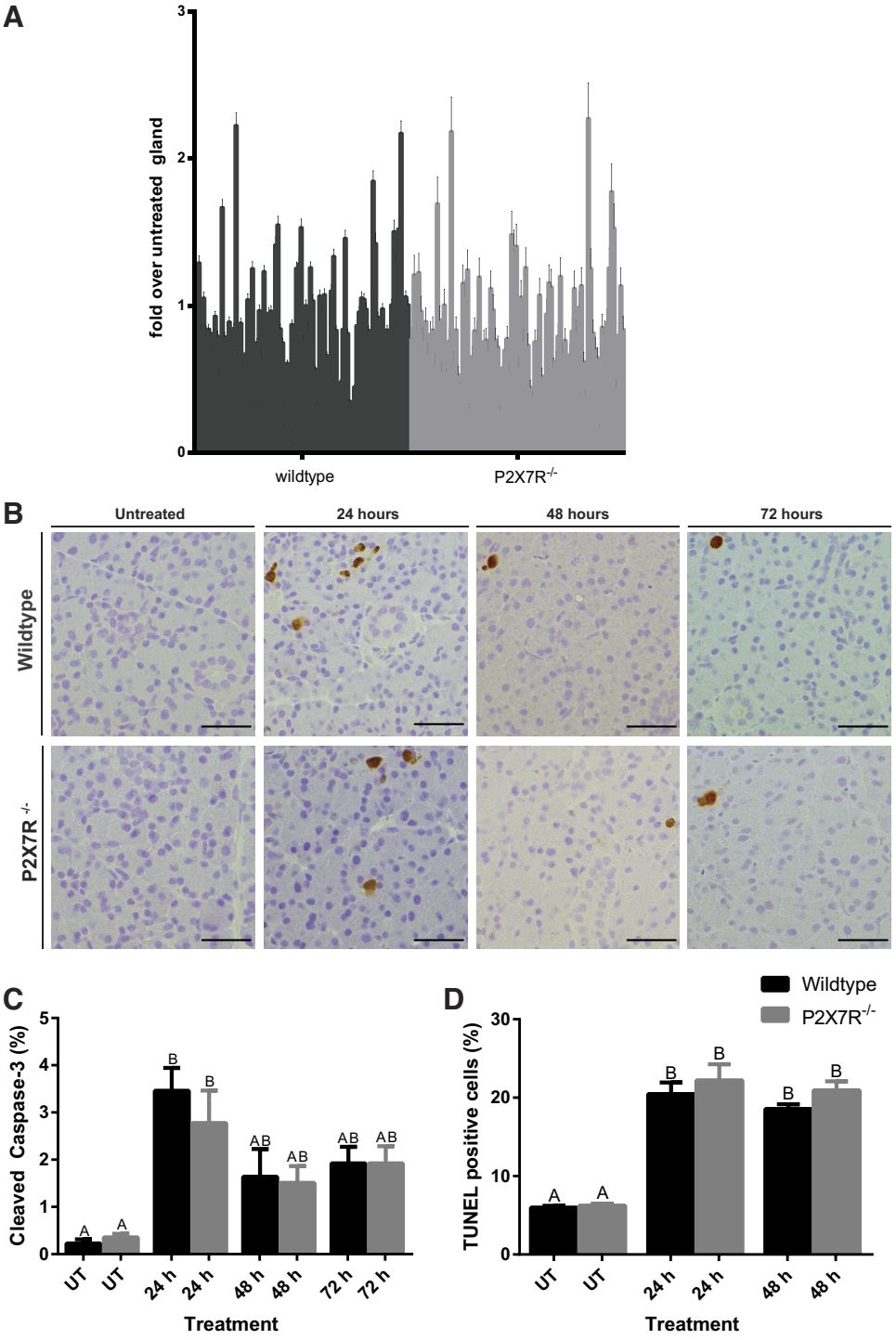

Fig. 2. P2X7 receptor (P2X7R) deletion does not prevent apoptosis following targeted head and neck γ-radiation in mice. P2X7R$^{-/-}$ (gray bars) and wild-type mice (black bars) were untreated (UT) or exposed to 5 Gy of radiation, and their salivary glands were removed at 24, 48 or 72 h after treatment. *A*: microarray analysis was done after 48 h on 5 Gy-treated salivary glands of wild-type and P2X7R$^{-/-}$ mice, and no significant differences in gene expression were observed. *B* and *C*: immunohistochemical staining was done using an anti-cleaved caspase-3 antibody, and cleaved caspase-3-positive apoptotic cells were quantified. *B*: representative images of positive cleaved caspase-3 staining (×400 magnification; scale bar = 25 μm). *C*: graph represents the total number of cleaved caspase-3-positive cells as a percentage of the total cell number per field of view. Data represent means ± SE of results from 4 mice per group and 5 fields of view per mouse with approximately 600–800 cells per field of view. *D*: terminal deoxynucleotidyl transferase dUTP nick-end labeling (TUNEL) staining was done and apoptotic cells were quantified. Graph represents the number of TUNEL-positive cells as a percentage of the total cell number per field of view. Data represent means ± SE of results from 4 mice per group and 3 fields of view per mouse with approximately 600–800 cells per field of view. *C* and *D*: normality was assessed using the Shapiro-Wilk test and significant differences were determined using one-way ANOVA and the Bonferroni post hoc test ($P < 0.05$). Data from treatment groups with the same letter are not significantly different from each other, but groups with different letters are significantly different.

for 1 h before γ-radiation treatment (10). Results show the concentration of eATP released from nonirradiated vehicle-treated (UT + Vehicle) and nonirradiated antagonist-treated cells (UT + Antagonist) is not significantly different (Fig. 1*B*). The eATP concentration is significantly increased in irradiated vehicle-treated cells (5 Gy + Vehicle) when compared with nonirradiated vehicle-treated cells (UT + Vehicle, Fig. 1*B*, $P < 0.01$), while the eATP concentration in irradiated antagonist-treated cells (5 Gy + Antagonist) is not different from nonirradiated antagonist-treated cells (UT + Antagonist) or nonirradiated vehicle-treated cells (UT + Vehicle). Therefore, P2X7R deletion or inhibition reduces γ-radiation-induced ATP release in primary parotid cells.

Cell apoptosis in irradiated parotid glands is similar between P2X7R$^{-/-}$ and wild-type mice. Prolonged P2X7R activation and increased ATP release often lead to cell death via apoptosis (1). In addition, apoptosis following radiation plays a key role in salivary gland dysfunction (8). The impact of P2X7R deletion on apoptotic signaling following γ-radiation was assessed using an apoptosis regulatory gene array with parotid tissues from wild-type and P2X7R$^{-/-}$ mice (48 h; 5 Gy). Of the 92 genes analyzed, there are no significant differences in RNA expression between groups (Fig. 2*A*). To determine the extent of apoptosis, parotid tissue sections from untreated or irradiated wild-type and P2X7R$^{-/-}$ mice were evaluated for cleaved caspase-3 by immunohistochemistry at 24, 48, and 72 h post-treatment. At 24 h after 5 Gy of radiation, the percentage of cleaved-caspase-3-positive cells is significantly increased in P2X7R$^{-/-}$ and wild-type mice compared with untreated controls (Fig. 2, *B* and *C*, $P < 0.05$). At subsequent time points postradiation, the level of apoptosis (i.e., cleaved-caspase 3) is not significantly different from untreated controls in either mouse model (Fig. 2*C*). To further evaluate radiation-induced cell apoptosis, TUNEL staining was performed on parotid tissue sections of untreated and irradiated mice at 24 and 48 h posttreatment. The percentage of TUNEL-positive cells increases at 24 and 48 h after 5 Gy of γ-radiation ($P < 0.001$), as compared with untreated controls and is not different between genotypes at any time point measured (Fig. 2*D*). These data suggest that P2X7R deletion does not impact the induction of apoptosis in salivary glands following γ-radiation.

Primary parotid cells from P2X7R$^{-/-}$ mice have reduced PGE$_2$ release following γ-radiation. PGE_2 is an arachidonic acid derivative secreted during inflammation and released following caspase-3 cleavage (2, 12) and P2X7R activation (5). To determine the amount of PGE_2 released from salivary glands after γ-radiation, primary parotid gland cells from P2X7R$^{-/-}$ and wild-type mice were irradiated and PGE_2 levels in the supernatant were determined by ELISA at 0, 24, 48, and 72 h. Primary parotid cells from untreated wild-type mice secrete 20-fold more PGE_2 compared with untreated P2X7R$^{-/-}$ primary cells (2,312 and 112 pg/ml, respectively, $P < 0.01$, Fig. 3*A*). Following radiation, there is 2.5- to 6.5-fold increase in PGE_2 release from wild-type primary cells over time (24 h: 5,829 pg/ml; 48 h: 9,366 pg/ml; and 72 h: 15,382 pg/ml, $P < 0.01$, Fig. 3*A*), as compared with untreated controls (2,312 pg/ml). In contrast, there is no significant increase in γ-radiation-induced PGE_2 release in P2X7R$^{-/-}$ primary cells at the time points evaluated (Fig. 3*A*). To confirm that the elevated levels of PGE_2 release in untreated wild-type cells was due to P2X7R activation, cells were treated with 10, 25, or 50 μM of the P2X7R antagonist A438079 for 1 or 24 h. PGE_2 release is significantly decreased following A438079 treatment at all concentrations of A438079 when compared with untreated controls (Fig. 3*B*, $P < 0.01$). These data suggest that P2X7R expression plays a critical role in PGE_2 secretion caused by γ-radiation in primary parotid gland cells.

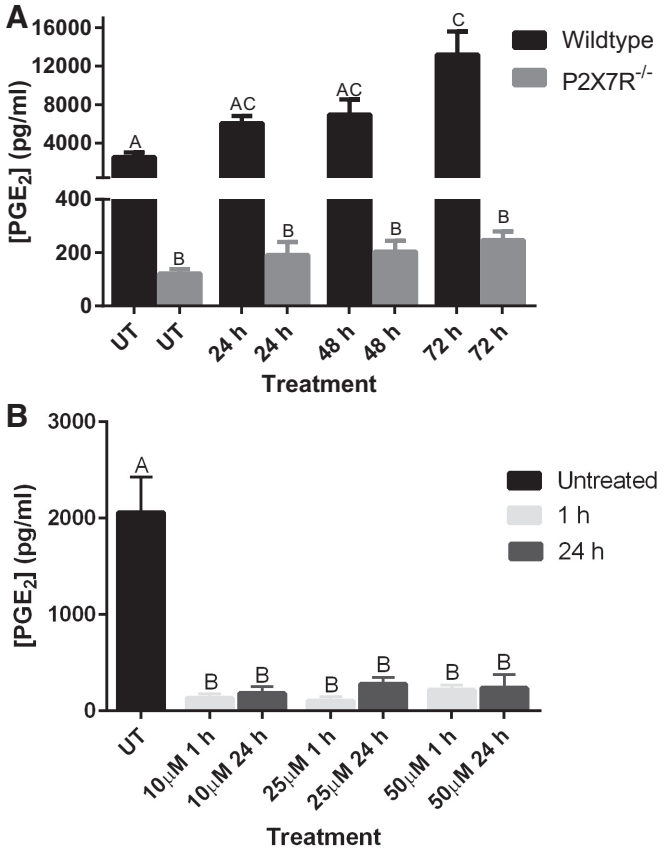

Fig. 3. P2X7 receptor (P2X7R) deletion decreases PGE_2 release from irradiated primary parotid gland cells. *A*: parotid gland cells were prepared, as described in MATERIALS AND METHODS, from P2X7R$^{-/-}$ (gray bars) and wild-type mice (black bars) and were untreated (UT; $n = 8$) or exposed to a single dose of 5 Gy of radiation. Supernatants were collected at 24, 48, and 72 h post-γ-radiation ($n = 5$ per treatment). *B*: wild-type primary cells were untreated (black bar, $n = 9$) or treated with 10, 25, or 50 μM of the P2X7R antagonist A438079 for 1 h (light gray bars, $n = 5$ per treatment) or 24 h (dark gray bars, $n = 5$ per treatment). PGE_2 content was determined via an enzyme-linked immunosorbent assay. *A* and *B*: data are presented as means ± SE. Normality was assessed with the Kolmogorov-Smirnov test on log-transformed data and significant differences were determined using one-way ANOVA and the Bonferroni post hoc test ($P < 0.05$). Data from treatment groups with the same letter are not significantly different from each other, but groups with different letters are significantly different.

Expression and activity of cyclooxygenase and PGE synthase isoforms are similar between P2X7R$^{-/-}$ and wild-type mice following γ-radiation. The conversion of arachidonic acid to PGE_2 occurs in a two-step process, requiring the activation of COX-1 or COX-2 to generate PGH_2 that is next converted to PGE_2 by three isoforms of PGE synthase: mPGES-1, mPGES-2, and cPGES. In general, COX-2 and mPGES-1 expression can be induced by inflammation, whereas COX-1, mPGES-2, and cPGES are constitutively expressed in most cell types (21). The expression level of each enzyme was determined via RT-PCR in parotid glands of wild-type and P2X7R$^{-/-}$ mice at 0, 24, and 48 h postradiation. For inducible mPGES-1 and

COX-2, only COX-2 expression was significantly increased in wild-type parotid glands 48 h post-γ-radiation, as compared with untreated controls (Fig. 4, *A* and *B*, $P < 0.05$). P2X7R deletion has minimal effects on mPGES-1 and COX-2 expression, albeit there is a transient decrease in mPGES-1 at 24 h post-γ-radiation. COX-1, mPGES-2, and cPGES are known to be constitutively expressed in various tissues, but this does not appear to be the case for irradiated salivary glands (Fig. 4, *C–E*). Both mPGES-2 and cPGES are decreased in parotid glands 24–48 h postradiation irrespective of mouse genotype. In contrast, COX-1 is significantly increased in wild-type parotid glands 48 h post-γ-radiation and significantly decreased in P2X7R$^{-/-}$ parotid glands 24–48 h postradiation, as compared with wild-type mice (Fig. 4*E*, $P < 0.01$). To further assess the role of this pathway, a cyclooxygenase activity assay kit was used to determine the extent of COX-1 and COX-2 activity in vivo. Surprisingly, the activity of inducible COX-2 is not different between genotypes or untreated and irradiated mice at any time point (Fig. 4*F*). COX-1 activity is significantly increased in P2X7R$^{-/-}$ mice at 48 h postradiation, as compared with wild-type mice (Fig. 4*G*, $P < 0.05$). These data indicate that alterations in expression or activities of cyclooxygenase or PGE synthase alone do not explain the differences in radiation-induced PGE_2 release between the two genotypes.

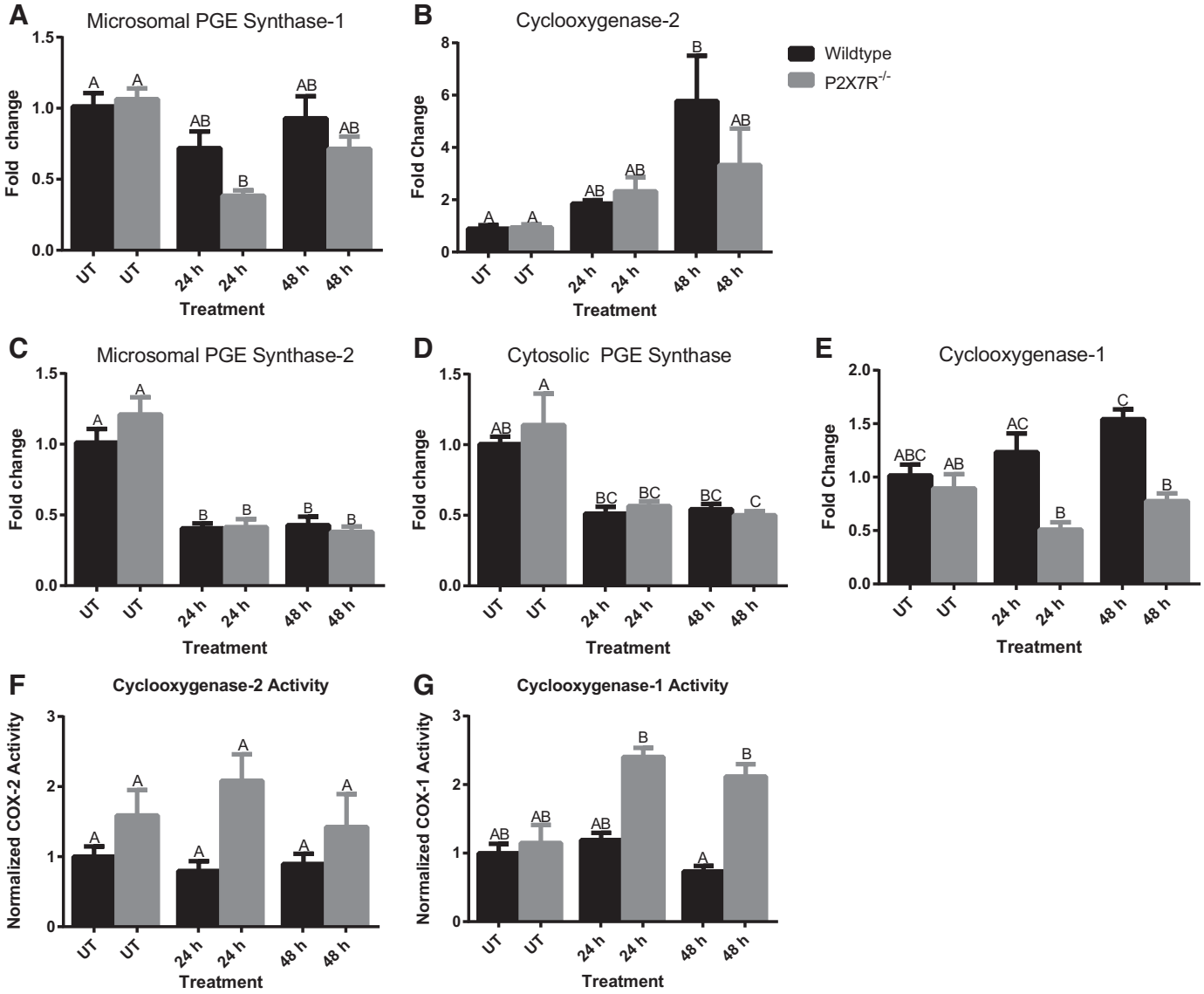

Fig. 4. Cyclooxygenase and PGE synthase isoform mRNA expression and cyclooxygenase isoform activities in parotid glands of wild-type and P2X7R$^{-/-}$ mice following γ-radiation. P2X7R$^{-/-}$ mice (gray bars) and wild-type mice (black bars) were untreated (UT) or exposed to 5 Gy of radiation and parotid glands were removed at 24 or 48 h after treatment. *A–E*: cDNA was prepared from parotid glands, as described in MATERIALS AND METHODS, and quantitative RT-PCR was performed with primers specific for *microsomal PGE-synthase-1* (*A*), *cyclooxygenase-2* (*B*), *microsomal PGE synthase-2* (*C*), *cytosolic PGE synthase* (*D*), and *cyclooxygenase-1* (*E*). Data were normalized to 15S ribosomal RNA as an internal control, and fold change was calculated relative to mRNA content in untreated wild-type mice. *F* and *G*: protein was extracted from parotid glands and cyclooxygenase enzyme activity was measured with a cyclooxygenase activity assay kit, as described in MATERIALS AND METHODS, for cyclooxygenase-2 (*F*) and cyclooxygenase-1 (*G*). *A–E*: normality was assessed using the Shapiro-Wilk test, and significant differences were determined using a one-way ANOVA and the Bonferroni post hoc test ($P < 0.05$). *F* and *G*: nonnormally distributed data were assessed with the Kruskal-Wallis test followed by Dunn's comparisons ($P < 0.05$). *A–G*: data are presented as means ± SE of results from 4 mice per treatment. Treatment groups with the same letter are not significantly different from each other, but groups with different letters are significantly different.

P2X7R deletion and antagonism prevent loss of salivary flow following γ-radiation. Alterations in salivary gland function are observed as early as 3 days following γ-radiation and persist chronically (8). To determine the role of the P2X7R in salivary gland radiosensitivity, we compared carbachol-stimulated salivary flow rates of P2X7R$^{-/-}$ and wild-type mice after radiation. On *day 3* post-γ-radiation, wild-type mice have a 30% decrease in saliva flow compared with untreated wild-type mice ($P < 0.05$), whereas saliva flow in irradiated P2X7R$^{-/-}$ mice is not significantly different from untreated P2X7R$^{-/-}$ or wild-type mice (Fig. 5*A*). On *day 30*, irradiated wild-type mice maintain a significant decrease (26%, $P < 0.05$) in salivary output compared with untreated wild-type mice (Fig. 5*B*). Conversely, salivary output in irradiated P2X7R$^{-/-}$ mice is not significantly different from untreated P2X7R$^{-/-}$ or wild-type mice, although it is significantly higher than in irradiated wild-type mice (Fig. 5*B*, $P < 0.01$).

We next evaluated the impact of pharmacological P2X7R inhibition on salivary flow rates in irradiated wild-type mice using the P2X7R antagonist A438079. FVB mice were intraperitoneally injected with A438079 (70 mg/kg body wt) 1 h before γ-radiation, and carbachol-stimulated saliva was collected on *days 3* and *30* postradiation; multi-antagonist treated mice received additional injections of A438079 on *days 5* and *10* postradiation. On *day 3*, irradiated mice injected with vehicle (5 Gy + Vehicle) have a 50% reduction in salivary flow (Fig. 5*C* $P < 0.01$), whereas irradiated mice injected with P2X7R antagonist (5 Gy + Antagonist) have similar salivary flow rates to both untreated groups. On *day 30*, irradiated mice injected with vehicle maintain ~50% reduction in saliva flow, as compared with untreated controls (Fig. 5*D*, $P < 0.01$), whereas irradiated mice injected with a single dose of A438079 (5 Gy + Antagonist) exhibit an ~40% reduction in stimulated saliva flow rates that is similar to irradiated mice injected with vehicle (Fig. 5*D*). Irradiated mice that received two additional injections of A438079 on *days 5* and *10* post-γ-radiation (5 Gy + multi-antagonist) had salivary outputs that were not different from either untreated group and were significantly increased compared with the other irradiated groups (Fig. 5*D*, $P < 0.01$). Therefore, one injection of the P2X7R antagonist 1 h before γ-radiation was able to preserve stimulated salivary flow rates at an acute time point (*day 3*), but multiple injections of the P2X7R antagonist pre- and postradiation were needed to reverse chronic loss of saliva secretion (*day 30*). These data strongly suggest that the P2X7R facilitates loss of salivary gland function following γ-radiation and that multiple doses of P2X7R antagonist can prevent γ-radiation-induced chronic hyposalivation.

P2X7R deletion does not alter the structural morphology of salivary glands. Hematoxylin and eosin-stained sections of multiple salivary glands (submandibular, parotid, and sub-

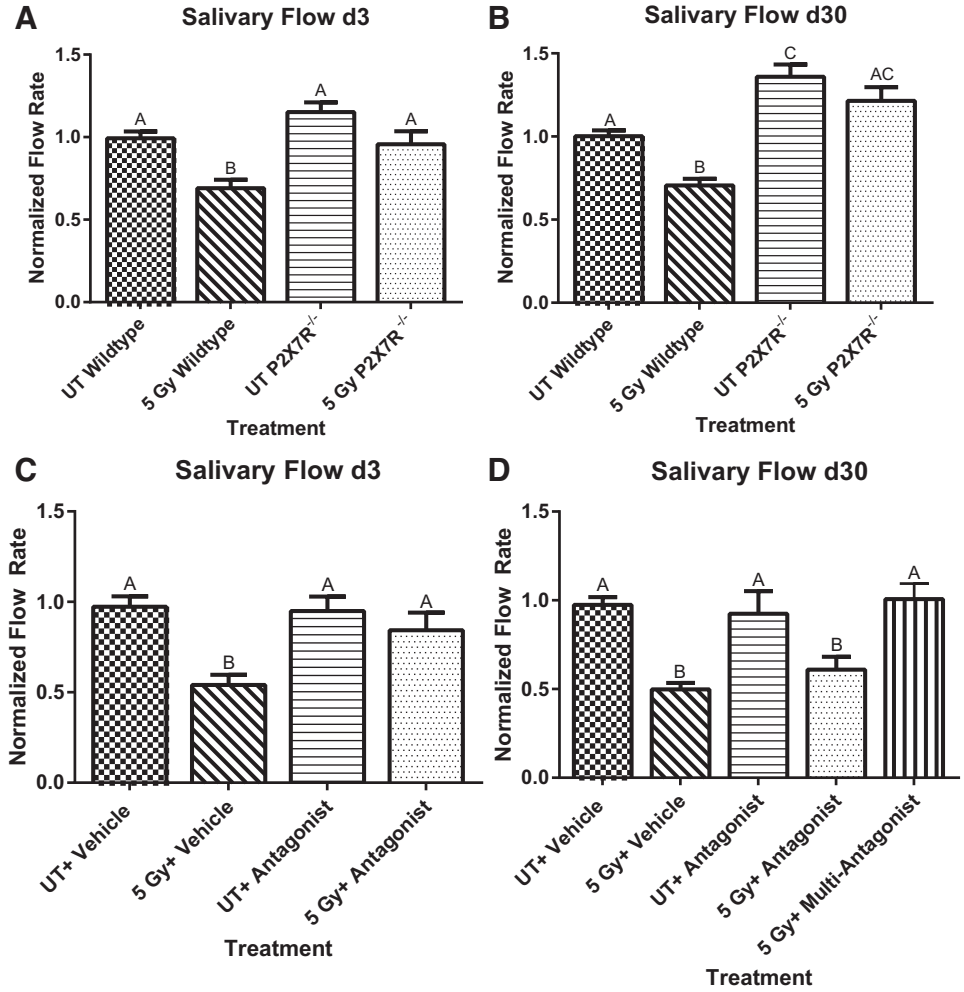

Fig. 5. P2X7 receptor (P2X7R) deletion or antagonism reverses loss of saliva secretion caused by targeted head and neck γ-radiation. *A* and *B*: wild-type (checkered bars, $n = 8$, diagonal-lined bars, $n = 9$) and P2X7R$^{-/-}$ mice (horizontal lined bars, $n = 10$, dotted bars, $n = 9$) were untreated (UT) or exposed to a single dose of 5 Gy of radiation and carbachol-stimulated (0.25 mg/kg body wt) saliva flow was measured on *day 3* (d3; *A*) and *day 30* (d30; *B*) postradiation, as described in MATERIALS AND METHODS. *C* and *D*: FVB mice were injected with saline (checkered bars, $n = 25$; diagonal lined bars, $n = 13$) or the P2X7R antagonist A438079 (70 mg/kg body weight; horizontal lined bars, $n = 15$; dotted bars, $n = 14$; vertical lined bars, $n = 9$) and 1 h later were left UT or exposed to a single dose of 5 Gy γ-radiation, as indicated. Multi-antagonist-treated mice also received A438079 injections (70 mg/kg) on *days 5* and *10* following radiation. *C* and *D*: saliva flow was measured on *day 3* (*C*) and *day 30* (*D*) *day 30* post-γ-radiation. Data are presented as means ± SE. Normality was assessed by the Kolmogorov-Smirnov test and significant differences were determined using one-way ANOVA and the Bonferroni post hoc test ($P < 0.05$). Data from treatment groups with the same letter are not significantly different from each other, but groups with different letters are significantly different.

lingual) from wild-type and P2X7R$^{-/-}$ mice were also evaluated for structural abnormalities. Untreated P2X7R$^{-/-}$ mice have no profound morphological differences compared with untreated wild-type mice (Fig. 6, *A–C*, *G*, and *H*). Thirty days post-γ-radiation, both wild-type and P2X7R$^{-/-}$ mice display mild atrophy of the salivary glands (Fig. 6, *D–F* and *J–L*).

DISCUSSION

Loss of salivary gland function after γ-radiation therapy is a serious side effect for many head and neck cancer patients that often persists for the remainder of their lives. There are currently no long-term treatment options available, and short-term options are relatively ineffective. In the present study, we determined the role of the P2X7R in radiation-induced salivary gland dysfunction and identified the receptor as a promising therapeutic target for preservation of secretory function. We found that P2X7R$^{-/-}$ mice maintained normal carbachol-stimulated salivary flow rates at *days 3* and *30* postradiation, which is equivalent to untreated P2X7R$^{-/-}$ or wild-type mice (Fig. 5, *A* and *B*). To test a potential therapeutic approach to prevent γ-radiation-induced salivary gland damage, we determined that a single injection of the P2X7R antagonist A438079 (70 mg/kg) preserved salivary function through *day 3* postradiation (Fig. 5*C*), but multiple injections of A438079 (pre- and postradiation) maintained function long term (30 days, Fig. 5*D*). Interestingly, the increase in salivary flow seen in irradiated P2X7R$^{-/-}$ versus wild-type mice does not correlate with a reduction in cell apoptosis (Fig. 2, *B–D*), which is in contrast to other mouse models of radiation-induced salivary gland dysfunction (4, 14, 15, 18). This suggests that the P2X7R plays a role in the loss of saliva secretion independent or downstream of apoptosis.

Inflammatory disorders, such as RA and RBI are associated with elevated eATP levels (3, 35), the endogenous agonist of the P2X7R (1, 16). After γ-radiation, we observed that ATP release increases in a radiation dose-dependent manner in wild-type primary parotid cells but remains unchanged in P2X7R$^{-/-}$ cells (Fig. 1*A*). Furthermore, pretreatment of irradiated wild-type primary cells with the P2X7R antagonist A439079 decreases ATP release to levels similar to both untreated groups (Fig. 1*B*). The alterations in ATP release are likely due to the pore-forming properties of the P2X7R through association with pannexin hemichannels (22, 25) following repetitive or prolonged P2X7R activation, which enables the downhill movement of intracellular ATP across the plasma membrane (1, 6, 30). The sustained release of eATP caused by localized tissue damage and P2X7R activation likely signals cells downstream of the site of injury to amplify the inflammatory response (16, 31).

PGE_2 is an inflammatory eicosanoid derived from arachidonic acid via cyclooxygenase and PGE synthase activities.

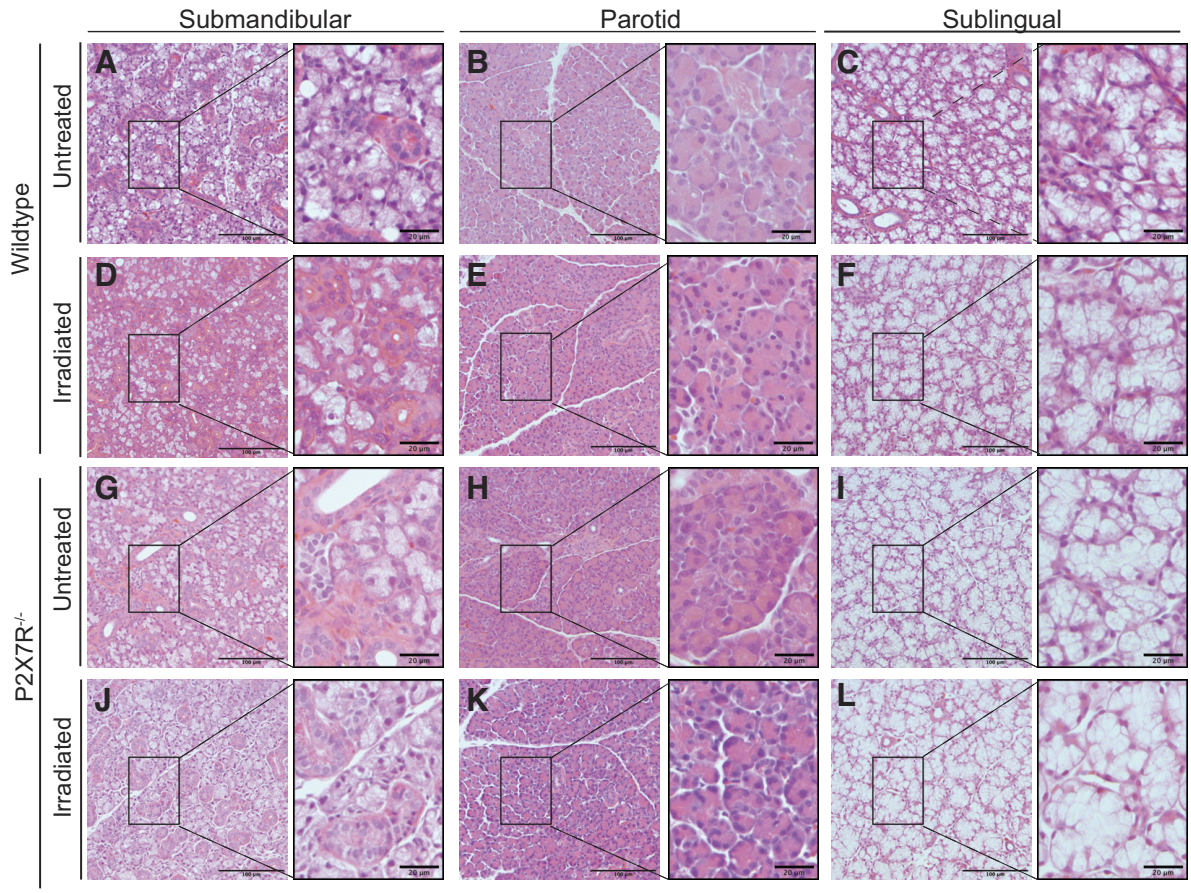

Fig. 6. Histological examination of salivary gland structure of untreated and irradiated P2X7R$^{-/-}$ and wild-type mice. *A–L*: sections of submandibular (*A*, *D*, *G*, and *J*), parotid (*B*, *E*, *H*, and *K*) or sublingual (*C*, *F*, *I*, and *L*) salivary glands were taken from untreated or 5-Gy-irradiated wild-type mice (*A–F*) or P2X7R$^{-/-}$ mice (*G–L*). Tissues were fixed in 10% (vol/vol) formalin, sectioned, stained with hematoxylin and eosin, and examined via bright-field microscopy at ×200 magnification. Scale bars = 100 μm (or 20 μm in boxed images).

Release of PGE_2 is dependent on caspase-3 and -7 activation following radiation of mouse embryonic fibroblasts (12). In the current study, γ-radiation of primary parotid cells from wild-type, but not $P2X7R^{-/-}$, mice caused a significant increase in PGE_2 release over 72 h (Fig. 3*A*). We anticipated that altered expression levels of either cyclooxygenase or PGE synthase isoforms would account for this increase in PGE_2 release, as COX-2 and mPGES-1 expression and activity are increased following inflammatory signals (21, 24). However, we detected only minimal differences in parotid gland mPGES-1 and COX-2 expression between wild-type and $P2X7R^{-/-}$ mice that would not account for the significant decrease in PGE_2 release during the radiation time course in cells from $P2X7R^{-/-}$ mice (Fig. 3 and Fig. 4, *A*, *B* and *F*). COX-1, mPGES-2 and cPGES expression levels were also similar between the two genotypes (Fig. 4, *C–E*). Interestingly, as compared with wild-type mice, COX-1 activity was increased in parotid glands of $P2X7R^{-/-}$ mice at 48 h post-γ-radiation (Fig. 4, *G*, $P < 0.05$), despite lower PGE_2 secretion in $P2X7R^{-/-}$ parotid cells (Fig. 3*A*) and lower parotid COX-1 mRNA expression (Fig. 4*E*). This observation could be explained by the fact that COX-1 converts arachidonic acid to PGH_2, which can then be converted to a number of bioactive lipids, such as prostacyclin, thromboxane, or prostaglandin D_2 (among others), depending on the enzyme that acts upon PGH_2 (24). Determining the role of each PGE synthase isoform in P2X7R-mediated PGE_2 release could be very informative, but such research is stymied by the lack of PGES isoform-specific inhibitors. Nonetheless, the data presented suggest that the marked decrease in PGE_2 release in parotid cells of $P2X7R^{-/-}$ mice postradiation is not due to alterations in the expression or activity of enzymes necessary for PGE_2 synthesis.

It has been shown that prolonged or repetitive P2X7R activation causes exosome release (31) and PGE_2 secretion occurs following P2X7R activation in macrophages, osteocytes and chondrocytes (5, 9, 13). Furthermore, previous research on P2Y receptors has shown that G_q protein-coupled $P2Y_2$ receptor ($P2Y_2R$) activation by eATP increases COX activity and secretion of prostacyclin (PGI_2) and PGE_2 (17, 34). $P2Y_2R$ expression is increased following IL-1β stimulation (23) and IL-1β has been shown to be secreted following P2X7R activation (10). Therefore, increases in P2X7R-mediated PGE_2 release observed post-γ-radiation may occur via IL-1β-induced upregulation of the $P2Y_2R$, a signaling pathway that would likely be inactive in $P2X7R^{-/-}$ mice.

In conclusion, we have shown that the P2X7R plays a role in γ-radiation-induced damage to salivary glands independent or downstream of apoptosis and may involve PGE_2 release. Importantly, our data show that antagonism of the P2X7R appears to be a viable therapeutic option for preventing salivary gland dysfunction in head and neck cancer patients undergoing γ-radiation treatment.

Perspectives and Significance

Despite technological advances in treatments for head and neck cancer, a significant number of patients continue to suffer from the side effects of normal tissue collateral damage during treatment. Previous studies have shown that reducing apoptotic cell death following radiation leads to preservation of salivary gland exocrine function; however, findings from the current study suggest that how the tissue responds to apoptotic cells may also be playing a critical role in radiation-induced salivary gland dysfunction. Release of prostaglandin E_2 has been shown to be downstream of caspase-3 activation, and this work demonstrates that the P2X7R can regulate this aspect of the inflammatory response induced by radiation. Understanding the downstream signaling cascades that are activated following apoptotic cell clearance and prostaglandin E_2 release may uncover mechanisms that lead to alternative avenues of normal tissue protection in patients receiving radiotherapy.

ACKNOWLEDGMENTS

We thank Grace Hill and Maricela Pier for technical assistance.

GRANTS

This work was supported by the National Institute of Dental and Craniofacial Research Grant R01-DE-023342 (to K. H. Limesand and G. A. Weisman).

DISCLAIMERS

The funding agency had no role in study design, data collection and analysis, the decision to publish this study, or the preparation of the manuscript.

DISCLOSURES

No conflicts of interest, financial or otherwise, are declared by the authors.

AUTHOR CONTRIBUTIONS

K.E.G., J.M.C., G.A.W., and K.H.L. conceived and designed research; K.E.G. and J.M.C. performed experiments; K.E.G., J.M.C., R.R.K., Q.Z., G.A.W., and K.H.L. analyzed data; K.E.G., J.M.C., R.R.K., G.A.W., and K.H.L. interpreted results of experiments; K.E.G. and J.M.C. prepared figures; K.E.G. drafted manuscript; K.E.G., J.M.C., R.R.K., Q.Z., G.A.W., and K.H.L. edited and revised manuscript; K.E.G., J.M.C., R.R.K., G.A.W., and K.H.L. approved final version of manuscript.

REFERENCES

1. **Adinolfi E, Pizzirani C, Idzko M, Panther E, Norgauer J, Di Virgilio F, Ferrari D.** P2X(7) receptor: death or life? *Purinergic Signal* 1: 219–227, 2005. doi:10.1007/s11302-005-6322-x.
2. **Allen CP, Tinganelli W, Sharma N, Nie J, Sicard C, Natale F, King M III, Keysar SB, Jimeno A, Furusawa Y, Okayasu R, Fujimori A, Durante M, Nickoloff JA.** DNA damage response proteins and oxygen modulate prostaglandin E2 growth factor release in response to low and high LET ionizing radiation. *Front Oncol* 5: 260, 2015. doi:10.3389/fonc.2015.00260.
3. **Arulkumaran N, Unwin RJ, Tam FW.** A potential therapeutic role for P2X7 receptor (P2X7R) antagonists in the treatment of inflammatory diseases. *Expert Opin Investig Drugs* 20: 897–915, 2011. doi:10.1517/13543784.2011.578068.
4. **Avila JL, Grundmann O, Burd R, Limesand KH.** Radiation-induced salivary gland dysfunction results from p53-dependent apoptosis. *Int J Radiat Oncol Biol Phys* 73: 523–529, 2009. doi:10.1016/j.ijrobp.2008.09.036.
5. **Barberà-Cremades M, Baroja-Mazo A, Gomez AI, Machado F, Di Virgilio F, Pelegrín P.** P2X7 receptor-stimulation causes fever via PGE2 and IL-1β release. *FASEB J* 26: 2951–2962, 2012. doi:10.1096/fj.12-205765.
6. **Brandao-Burch A, Key ML, Patel JJ, Arnett TR, Orriss IR.** The P2X7 receptor is an important regulator of extracellular ATP levels. *Front Endocrinol (Lausanne)* 3: 41–50, 2012. doi:10.3389/fendo.2012.00041.
7. **Elliott MR, Chekeni FB, Trampont PC, Lazarowski ER, Kadl A, Walk SF, Park D, Woodson RI, Ostankovich M, Sharma P, Lysiak JJ, Harden TK, Leitinger N, Ravichandran KS.** Nucleotides released by apoptotic cells act as a find-me signal to promote phagocytic clearance. *Nature* 461: 282–286, 2009. doi:10.1038/nature08296.
8. **Grundmann O, Mitchell GC, Limesand KH.** Sensitivity of salivary glands to radiation: from animal models to therapies. *J Dent Res* 88: 894–903, 2009. doi:10.1177/0022034509343143.

9. **Hu H, Yang B, Li Y, Zhang S, Li Z.** Blocking of the P2X7 receptor inhibits the activation of the MMP-13 and NF-κB pathways in the cartilage tissue of rats with osteoarthritis. *Int J Mol Med* 38: 1922–1932, 2016. doi:10.3892/ijmm.2016.2770.
10. **Khalafalla MG, Woods LT, Camden JM, Khan AA, Limesand KH, Petris MJ, Erb L, Weisman GA.** P2X7 receptor antagonism prevents IL-1β release from salivary epithelial cells and reduces inflammation in a mouse model of autoimmune exocrinopathy. *J Biol Chem* 292: 16626–16637, 2017. doi:10.1074/jbc.M117.790741.
11. **Lenertz LY, Gavala ML, Hill LM, Bertics PJ.** Cell signaling via the P2X(7) nucleotide receptor: linkage to ROS production, gene transcription, and receptor trafficking. *Purinergic Signal* 5: 175–187, 2009. doi:10.1007/s11302-009-9133-7.
12. **Li F, Huang Q, Chen J, Peng Y, Roop DR, Bedford JS, Li CY.** Apoptotic cells activate the "phoenix rising" pathway to promote wound healing and tissue regeneration. *Sci Signal* 3: ra13, 2010. doi:10.1126/scisignal.2000634.
13. **Li J, Liu D, Ke HZ, Duncan RL, Turner CH.** The P2X7 nucleotide receptor mediates skeletal mechanotransduction. *J Biol Chem* 280: 42952–42959, 2005. doi:10.1074/jbc.M506415200.
14. **Limesand KH, Said S, Anderson SM.** Suppression of radiation-induced salivary gland dysfunction by IGF-1. *PLoS One* 4: e4663, 2009. doi:10.1371/journal.pone.0004663.
15. **Limesand KH, Avila JL, Victory K, Chang HH, Shin YJ, Grundmann O, Klein RR.** Insulin-like growth factor-1 preserves salivary gland function after fractionated radiation. *Int J Radiat Oncol Biol Phys* 78: 579–586, 2010. doi:10.1016/j.ijrobp.2010.03.035.
16. **Lister MF, Sharkey J, Sawatzky DA, Hodgkiss JP, Davidson DJ, Rossi AG, Finlayson K.** The role of the purinergic P2X7 receptor in inflammation. *J Inflamm (Lond)* 4: 5, 2007. doi:10.1186/1476-9255-4-5.
17. **Lustig KD, Erb L, Landis DM, Hicks-Taylor CS, Zhang X, Sportiello MG, Weisman GA.** Mechanisms by which extracellular ATP and UTP stimulate the release of prostacyclin from bovine pulmonary artery endothelial cells. *Biochim Biophys Acta* 1134: 61–72, 1992. doi:10.1016/0167-4889(92)90028-A.
18. **Martin KL, Hill GA, Klein RR, Arnett DG, Burd R, Limesand KH.** Prevention of radiation-induced salivary gland dysfunction utilizing a CDK inhibitor in a mouse model. *PLoS One* 7: e51363, 2012. doi:10.1371/journal.pone.0051363.
19. **McGaraughty S, Chu KL, Namovic MT, Donnelly-Roberts DL, Harris RR, Zhang XF, Shieh CC, Wismer CT, Zhu CZ, Gauvin DM, Fabiyi AC, Honore P, Gregg RJ, Kort ME, Nelson DW, Carroll WA, Marsh K, Faltynek CR, Jarvis MF.** P2X7-related modulation of pathological nociception in rats. *Neuroscience* 146: 1817–1828, 2007. doi:10.1016/j.neuroscience.2007.03.035.
20. **Morgan-Bathke M, Hill GA, Harris ZI, Lin HH, Chibly AM, Klein RR, Burd R, Ann DK, Limesand KH.** Autophagy correlates with maintenance of salivary gland function following radiation. *Sci Rep* 4: 5206, 2014. doi:10.1038/srep05206.
21. **Park JY, Pillinger MH, Abramson SB.** Prostaglandin E2 synthesis and secretion: the role of PGE2 synthases. *Clin Immunol* 119: 229–240, 2006. doi:10.1016/j.clim.2006.01.016.
22. **Pelegrin P, Surprenant A.** Pannexin-1 mediates large pore formation and interleukin-1beta release by the ATP-gated P2X7 receptor. *EMBO J* 25: 5071–5082, 2006. doi:10.1038/sj.emboj.7601378.
23. **Peterson TS, Thebeau CN, Ajit D, Camden JM, Woods LT, Wood WG, Petris MJ, Sun GY, Erb L, Weisman GA.** Up-regulation and activation of the $P2Y_{(2)}$ nucleotide receptor mediate neurite extension in IL-1β-treated mouse primary cortical neurons. *J Neurochem* 125: 885–896, 2013. doi:10.1111/jnc.12252.
24. **Ricciotti E, FitzGerald GA.** Prostaglandins and inflammation. *Arterioscler Thromb Vasc Biol* 31: 986–1000, 2011. doi:10.1161/ATVBAHA.110.207449.
25. **Savio LE, de Andrade Mello P, da Silva CG, Coutinho-Silva R.** The P2X7 receptor in inflammatory diseases: angel or demon? *Front Pharmacol* 9: 52, 2018. doi:10.3389/fphar.2018.00052.
26. **Siegel RL, Miller KD, Jemal A.** Cancer statistics, 2018. *CA Cancer J Clin* 68: 7–30, 2018. doi:10.3322/caac.21442.
27. **Trautmann A.** Extracellular ATP in the immune system: more than just a "danger signal". *Sci Signal* 2: pe6, 2009. doi:10.1126/scisignal.256pe6.
28. **Tsukimoto M, Homma T, Ohshima Y, Kojima S.** Involvement of purinergic signaling in cellular response to gamma radiation. *Radiat Res* 173: 298–309, 2010. doi:10.1667/RR1732.1.
29. **Wang Q, Wang L, Feng YH, Li X, Zeng R, Gorodeski GI.** P2X7 receptor-mediated apoptosis of human cervical epithelial cells. *Am J Physiol Cell Physiol* 287: C1349–C1358, 2004. doi:10.1152/ajpcell.00256.2004.
30. **Weisman GA, Dé BK, Friedberg I, Pritchard RS, Heppel LA.** Cellular responses to external ATP which precede an increase in nucleotide permeability in transformed cells. *J Cell Physiol* 119: 211–219, 1984. doi:10.1002/jcp.1041190211.
31. **Wiley JS, Sluyter R, Gu BJ, Stokes L, Fuller SJ.** The human P2X7 receptor and its role in innate immunity. *Tissue Antigens* 78: 321–332, 2011. doi:10.1111/j.1399-0039.2011.01780.x.
32. **Woods LT, Camden JM, Batek JM, Petris MJ, Erb L, Weisman GA.** P2X7 receptor activation induces inflammatory responses in salivary gland epithelium. *Am J Physiol Cell Physiol* 303: C790–C801, 2012. doi:10.1152/ajpcell.00072.2012.
33. **Xie Y, Williams CD, McGill MR, Lebofsky M, Ramachandran A, Jaeschke H.** Purinergic receptor antagonist A438079 protects against acetaminophen-induced liver injury by inhibiting p450 isoenzymes, not by inflammasome activation. *Toxicol Sci* 131: 325–335, 2013. doi:10.1093/toxsci/kfs283.
34. **Xu J, Chalimoniuk M, Shu Y, Simonyi A, Sun AY, González FA, Weisman GA, Wood WG, Sun GY.** Prostaglandin E_2 production in astrocytes: regulation by cytokines, extracellular ATP, and oxidative agents. *Prostaglandins Leukot Essent Fatty Acids* 69: 437–448, 2003. doi:10.1016/j.plefa.2003.08.016.
35. **Xu P, Xu Y, Hu B, Wang J, Pan R, Murugan M, Wu LJ, Tang Y.** Extracellular ATP enhances radiation-induced brain injury through microglial activation and paracrine signaling via P2X7 receptor. *Brain Behav Immun* 50: 87–100, 2015. doi:10.1016/j.bbi.2015.06.020.